

Integrated electrocatalytic processing of levulinic acid and formic acid to produce biofuel intermediate valeric acid†

Cite this: *Green Chem.*, 2014, **16**, 1305

Yang Qiu,^{‡a} Le Xin,^{‡a} David J. Chadderdon,^a Ji Qi,^a Changhai Liang^b and Wenzhen Li^{*a}

Herein, we report integrated electrocatalytic processing of simulated acid-catalyzed cellulose hydrolysis downstream (levulinic acid + formic acid) to the biofuel intermediate valeric acid (VA). This green electro-biorefining process does not require complex steps to separate levulinic acid and formic acid (FA) from H₂SO₄; instead it couples electrocatalytic hydrogenation (ECH) of levulinic acid (LA) in a single electrocatalytic flow cell reactor and electrocatalytic oxidation of formic acid in a proton exchange membrane-direct formic acid fuel cell (DFAFC). The presence of FA has shown no negative effect on the ECH of LA and a high VA selectivity of >90% can be achieved on a non-precious Pb electrode while the Faradaic efficiency remains >47% during 8 hours of reaction in the single electrocatalytic flow cell reactor. This stream is fed directly to the DFAFC with a Pd/C anode catalyst to self-sustainably remove FA where 47% conversion of FA can be reached in 6 hours. However, electro-oxidation of FA over Pd/C appears to be reversibly inhibited by the product VA produced during ECH of LA. The electro-oxidation of FA + C₂–C₅ alkyl carboxylic acid in the half cell study shows that such an inhibition effect could have originated from the –COOH adsorption on the Pd surface. Higher carboxylic acid concentration and longer carbon chain lead to more serious loss of the electrocatalytic surface area (ECSA) of Pd/C.

Received 1st November 2013,
Accepted 20th November 2013

DOI: 10.1039/c3gc42254b

www.rsc.org/greenchem

Introduction

With the world population rapidly increasing and major crude oil reserves diminishing, our present unsustainable energy situation of heavy reliance on fossil fuels has to be changed.^{1–3} Seeking renewable energy resources is of critical importance, and thus has attracted enormous R&D attention worldwide.^{4–6} Abundant and renewable ligno-cellulosic biomass is expected to occupy a significant position in our future energy landscape; thus it has great potential to serve as feedstock to produce chemicals, polymers, and biofuels.^{4,7,8} One of the most important components derived from ligno-cellulosic biomass is highly polymerized cellulose (DP 7000–15 000), which can be employed as a sustainable source to produce levulinic acid (LA) through dilute acid-catalyzed hydrolysis processes.^{4,9,10} Levulinic

acid can be further upgraded to a wide range of value-added chemicals and fuel additives,^{9,11} and has been identified as one of the top abundant, renewable building-block biomass compounds by the US-DOE.¹² The hydrolysis of waste cellulose to levulinic acid is carried out in 0.1–0.5 M sulfuric acid aqueous solution; equal molar levulinic acid and formic acid (mol_{FA} : mol_{LA} = 1 : 1) can be cheaply produced at yields of 70% and 50%, respectively.^{13,14}

Unfortunately, both the by-product FA and the residual sulfuric acid that remained in the hydrolysis downstream will bring some complexities to the subsequent transformation of LA to biodegradable chemicals or fuel additives during heterogeneous catalytic processes.^{9,14,15} It has been reported that FA can rapidly deactivate the noble metal catalysts, and has negative effects on de-oxygenation of LA. For example, fed with an LA + FA mixture stream, gamma-valerolactone (gVL) was produced in low yield over Ru/C, which was mainly due to the poisoning effect of FA.^{16,17} Thus, novel processing routes and advanced catalysts have recently been explored to remove or utilize the by-product FA. For example, a continuous dual bed tubular reactor was developed where Ru-P/SiO₂ and Ru/TiO₂ catalysts fixed separately in this two-stage process are responsible for the decomposition of FA and hydrogenation of LA, respectively.¹⁷ Dumesic and co-workers have also designed

^aDepartment of Chemical Engineering, Michigan Technological University, Houghton, Michigan, USA. E-mail: wzli@mtu.edu; Fax: +1-906-487-3213; Tel: +1-906-487-2298

^bState Key Laboratory of Fine Chemicals, School of Chemical Engineering, Dalian University of Technology, Dalian, Liaoning, China

†Electronic supplementary information (ESI) available. See DOI: 10.1039/c3gc42254b

‡These authors contributed equally to this work.

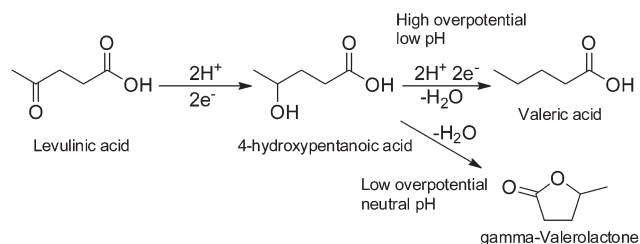
bimetallic RuSn₄/C and RuRe (3:4)/C catalysts that demonstrate sufficient stability to tolerate acidic conditions for gVL synthesis, through which LA together with FA can be fed into the reactor and FA is directly self-decomposed to CO₂ and H₂.^{18,19} It not only successfully utilizes the formic acid as a hydrogen source, avoiding the external petroleum-derived hydrogen supply, but also mitigates the greenhouse gas emission, because the generated CO₂ can be effectively captured and treated for other applications.^{20,21} The residual sulfuric acid in the downstream has also been found to deteriorate the metallic catalysts for hydrogenation of the LA to gVL;^{22,23} thus, novel processes need to be developed to separate LA and FA from aqueous sulfuric acid. Direct esterification of LA and FA using alcohols and butane has been developed to produce hydrophobic LA and FA ester, which automatically separate from residual aqueous sulfuric acid, and can then be recycled for cellulose dehydration.^{24–27} Although the above mentioned processes directly used FA from hydrolysis of cellulose as a hydrogen source, high pressure H₂ is still required; this needs special hydrogen management and robust reactor design. In addition, the removal and reuse of H₂SO₄, despite providing possible solutions, still need the subsequent separation and recovery of target products, which accounts for a large portion of the working capital.²² Therefore, exploring alternative and sustainable strategies of upgrading the cellulose hydrolysis downstream to biofuel (intermediates) is still necessary to supplement the current heterogeneous catalytic hydrogenation processes.

Electrocatalysis has been investigated for the reduction of sugars and their downstream derivatives in dilute sulfuric acid solution, which serves as a hydrogen source (to provide H_{ads} atom).^{28,29} Altering the sulfuric acid concentration to control the acidity (pH) of feedstock solution was found to be capable of regulating product distributions for some electro-reduction reactions.³⁰ Our recent work has demonstrated that non-noble metal lead (Pb) provides an effective electrode material for LA reduction. LA is dominantly converted to gVL in neutral solution (pH = 7.5) while valeric acid (VA) is the main product of LA reduction in acid solution (pH = 0) on a Pb electrode (Scheme 1).³⁰ Therefore, sulfuric acid from the downstream of acid-catalyzed hydrolysis of cellulose can be directly used as a hydrogen source (supply of H_{ads} atoms) for selective electrocatalytic hydrogenation (ECH) of LA to VA or gVL. This green electrocatalytic reduction route has a big advantage of avoidance of

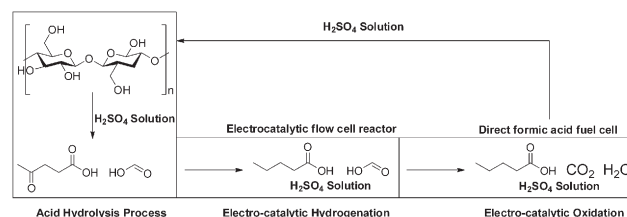
an energy-intensive separation process to remove the residual sulfuric acid. Interestingly, we also found that the applied potential is able to control the pathway of ECH of LA on a Pb electrode, and thus provides an effective means of obtaining desirable products. As shown in Scheme 1, the intermediate 4-hydroxypentanoic acid obtained from LA electro-reduction will be further hydrogenated to produce VA, or desorb from the catalyst surface to form gVL directly. It shows that high over-potential enables LA hydrogenation to VA with a high selectivity, while gVL is favorably produced at low overpotential. Under optimized conditions, we have demonstrated a high VA yield of >90% from ECH of LA with >86% Faradaic efficiency on a Pb electrode.

However, our previous work has only used pure biomass platform compound LA to demonstrate the feasibility of ECH in a single electrocatalytic flow cell reactor. It would be more desirable and practical to directly produce a biofuel intermediate (VA or gVL) from the ligno-cellulosic biomass hydrolysis downstream: LA with equal molar FA in sulfuric acid solution. Employing a proton exchange membrane-direct formic acid fuel cell (DFAFC) offers a great opportunity to not only remove FA to purify VA biofuel intermediate, but also simultaneously generate electrical energy to supplement the energy cost resulting from ECH of LA. Compared with liquid alcohol fuels, DFAFC has shown higher output electrical power density. It has been discovered that FA electro-oxidation on Pd-based catalysts proceeds primarily *via* the pathway without the formation of strongly poisoning CO intermediates and exhibits higher fuel cell performance than that on Pt.^{31–38} DFAFCs with Pd-based catalysts can yield very high power density under optimized test conditions, which has great potential for portable devices. Masel *et al.* have shown that a DFAFC with Pd black and Pd/C anode catalysts can reach a maximum power density of 243 mW cm⁻² and 171 mW cm⁻², respectively, with 3 M formic acid at 30 °C.^{31,32} Therefore, the output electrical energy generated from DFAFC with Pd-based anode catalysts can, presumably, efficiently and self-sustainably remove FA and meanwhile supply the portion of energy needed for ECH of LA.

Aiming at exploring a green electrocatalytic strategy to process realistic raw biomass feedstock, in this article, we studied coupling electrocatalytic hydrogenation of LA with electrocatalytic oxidation of FA by using the downstream of the acid-catalyzed cellulose hydrolysis process (LA + FA + sulfuric acid), as shown in Scheme 2. This integrated green



Scheme 1 Reaction scheme for the ECH of levulinic acid to valeric acid or gamma-valerolactone (gVL) on a Pb electrode.



Scheme 2 Schematic flow diagram of coupling of the single electrocatalytic flow cell reactor and DFAFC reactor, using the downstream of acid-catalyzed cellulose hydrolysis (LA + FA + H₂SO₄) as feedstock.

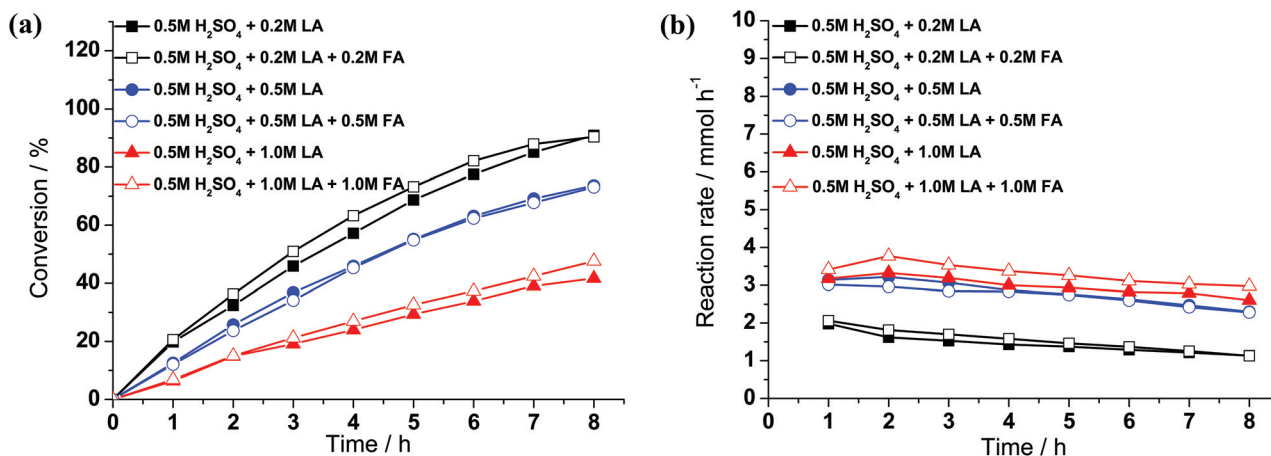


Fig. 1 (a) Conversion and (b) reaction rate of ECH of LA in 0.5 M H₂SO₄ aqueous solution at -1.5 V vs. RHE on a Pb electrode in an electrocatalytic flow cell reactor under ambient pressure and room temperature.

electrocatalytic process is attractive because it can upgrade LA to valeric biofuel intermediate at low electrical energy cost, while simultaneously removing FA. The bulk Pb electrode is employed as the cathode catalyst for the ECH of LA + FA in a single electrocatalytic flow cell reactor. We expect that formic acid is inert and has no negative effect on the ECH of LA. Subsequently, the products (VA + FA) aqueous solution is fed into DFAFC with the Pd/C anode catalyst to remove FA and generate electricity concurrently. In order to investigate the effects of the coupled components through this integrated process, the downstream of acid-catalyzed cellulose hydrolysis is simulated by equal molar LA and FA in sulfuric acid aqueous solution. The prospects and challenges of this integrated electrocatalytic bio-refining process are also discussed in this paper.

Results and discussion

Electrocatalytic hydrogenation of levulinic acid + formic acid

The aqueous-phase ECH of LA and LA + FA was carried out in a custom-designed single electrocatalytic flow cell reactor with a Pb electrode. LA and FA with a molar ratio of 1 : 1 in H₂SO₄ aqueous solution was circulated in a closed loop to the cathode chamber of the reactor at room temperature. As a control experiment, the same concentration of LA (0.2 M, 0.5 M, and 1.0 M) without the addition of FA was also tested under identical conditions. Our recent work has investigated the cyclic voltammograms (CV) of the ECH of LA on a Pb electrode in 0.5 M H₂SO₄. In the presence of 0.2 M LA, the onset potential is over 200 mV more positive and the cathodic reduction current is greater than that without LA. However, an optimized potential is required to yield a significant amount of target products at an appreciable rate.^{28,30,39,40} Thus, all the presented electrocatalysis studies are conducted at an optimized applied potential of -1.5 V vs. RHE, because as the applied potential is set more negative, the relative ECH rate

will decrease, making it less competitive for surface H atoms, and therefore the Faradaic efficiency will drop off.

Fig. 1 presents the LA conversion and reaction rate vs. time for various feed compositions over a Pb electrode in the proton exchange membrane (PEM)-based single electrocatalytic flow cell reactor. The reactant and products collected at certain time intervals were analysed by HPLC. Fig. 1(a) shows that LA conversions of 90.9%, 73.6% and 41.7% can be obtained after 8 hours electro-hydrogenation reaction with LA concentration fed at 0.2 M, 0.5 M and 1.0 M, respectively. The conversion decreases with the increase of the initial LA concentration, since the geometry of a Pb electrode involved in the catalytic process governs the electrocatalytic efficiency.⁴¹ In this respect, the active surface of a Pb electrode intimately interacting with the LA aqueous solution cannot provide sufficient reaction sites to afford hydrogenation of LA with higher concentrations. Nonetheless, the reaction rate of 0.5 M LA is generally higher than that of 0.2 M LA, as shown in Fig. 1(b). However, further increase of LA concentration to 1.0 M does not help to increase the reaction rate, which may be due to the insufficient quantity of adsorbed hydrogen for the complete hydrogenation of all the LA present in the solution. Importantly, it is demonstrated in Fig. 1 that both the conversion and reaction rate of LA do not decrease in the presence of FA in the course of 8 hours of reaction, suggesting that FA has no "inhibition effect" on LA hydrogenation. For example, fed with equal molar FA and LA mixture streams (0.2 M, 0.5 M and 1.0 M), LA conversion of 90.4%, 73.1% and 47.6% is desirably obtained; the results strongly resemble that of pure LA fed. In order to examine whether FA is nearly inert on a Pb electrode at an applied potential of -1.5 V (vs. RHE), we have quantified the FA concentration each hour using HPLC. As seen in Fig. 2, the FA concentration undergoes no significant change during the long run time. There are no unidentified side product peaks in the liquid chromatographs. The slight diminishing of FA concentration (*ca.* 10%) is probably a result of the evaporation of the FA during 8 hours of reaction, which can be supported by the

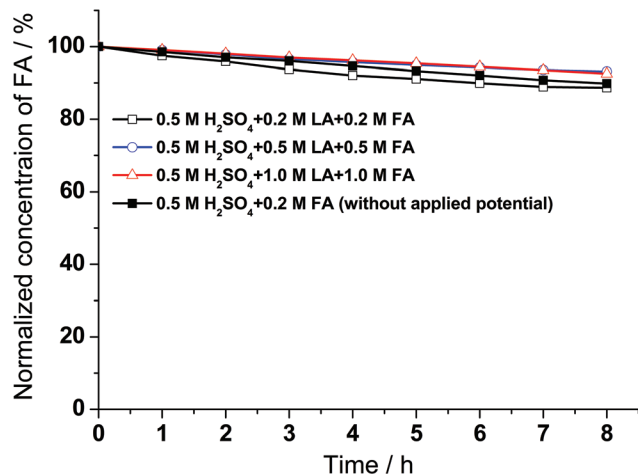


Fig. 2 Normalized concentration of FA during 8 hour ECH of LA at -1.5 V vs. RHE on a Pb electrode in an electrocatalytic flow cell reactor under ambient pressure and room temperature.

blank experiment without applying a potential of -1.5 V vs. RHE.

Furthermore, the selectivity of VA and gVL can be regulated by the applied potential (-1.5 V vs. RHE) and almost remains constant during the 8 hour reaction, as shown in Fig. 3. However, with the LA concentration increasing from 0.2 M to 1.0 M, the selectivity of VA decreases from 96.5% to 86.3%, while the selectivity of gVL increases from 3.5% to 13.7% (Fig. 3). At higher concentration of LA, protons in solution are presumably more quickly consumed for LA hydrogenation, resulting in the pH increasing near the cathode surface. Higher local pH likely affects the adsorption behavior and reaction energies of the substrates and makes the ECH of LA to VA *via* four-electron transfer relatively difficult (Scheme 1). While this pH regulation effect has been proposed in our recent publication,³⁰ we demonstrated here that the selectivity to VA can be slightly increased by co-feeding LA along with the FA,

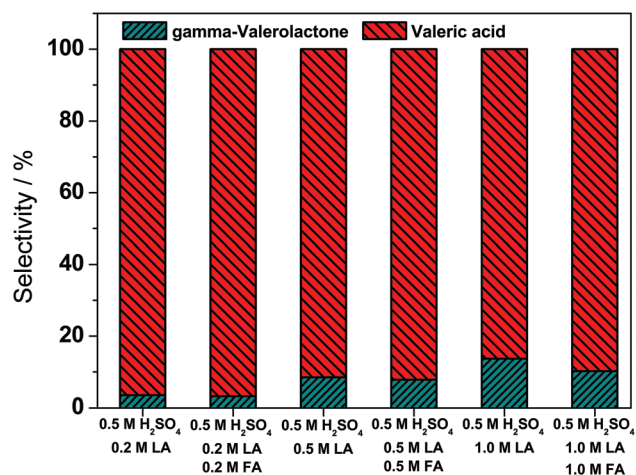


Fig. 3 Selectivity of ECH of LA at -1.5 V vs. RHE on a Pb electrode in an electrocatalytic flow cell reactor under ambient pressure and room temperature.

especially when a higher concentration of LA was employed. It is observed that the selectivity of VA ramps up from 86.3% in 1.0 M LA to 89.8% in 1.0 M LA + 1.0 M FA solution (Fig. 3). In the presence of strong sulfuric acid ($pK_a = -3$), formic acid ($pK_a = 3.77$) and levulinic acid ($pK_a = 4.59$) are preferably in neutral molecules without de-protonation in the aqueous solution. Therefore, we suggest that the amount of protons originating from FA is negligible; however, the presence of FA probably diluted the LA aqueous solution, so that the availability of adsorbed hydrogen in proximity to LA was enhanced, thus facilitating the conversion of LA to VA.

The Faradaic efficiency (FE) represents the competition between the electrocatalytic hydrogenation (ECH) and the hydrogen gas evolution reaction (HER). In general, FE drops gradually in the course of ECH of LA, regardless of the different compositions of LA solutions introduced into the system, as shown in Fig. 4. It indicates that a larger fraction of the current goes to generating hydrogen gas as more LA is converted. With the equal moles of FA added, no apparent change is observed regarding the FE for ECH of 0.2 M and 0.5 M LA, while the average FE increases by 4% when comparing 1.0 M LA without and with 1.0 M FA added. During the ECH of LA with higher concentration, higher current was observed, which accelerates the proton generation near the Pb electrode surface. Not only will it result in higher local pH and more gVL production, but also the overall reaction rate and efficiency are decreased. However, the replenishment of consumed protons in proximity to the surface due to the dilution by FA increases FE.

Taken together, the presence of FA in the LA aqueous solution has been found to have no negative effect on the ECH of LA in terms of conversion, reaction rate, selectivity, as well as FE. Although the detailed mechanisms of the role of FA in the ECH of LA are not very clear, the results show promise to upgrade the LA arising directly from the downstream of cellulose hydrolysis with sulfuric acid to provide an upstream (VA +

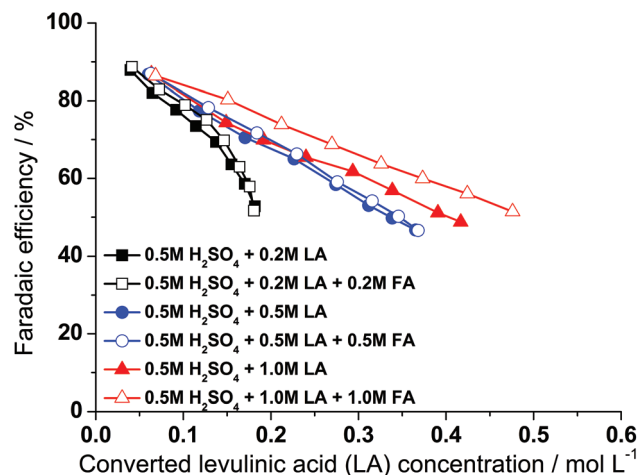


Fig. 4 Faradaic efficiency (FE) versus the converted LA concentration at -1.5 V vs. RHE on a Pb electrode in an electrocatalytic flow cell reactor under ambient pressure and room temperature.

LA + sulfuric acid) for subsequent electrocatalytic oxidation of FA to purify the biofuel intermediate VA.

Electrocatalytic oxidation of formic acid + valeric acid

It has been widely recognized that Pd is a more active catalyst toward electro-oxidation of formic acid due to its facilitating the direct 2-electron-transfer pathway. Our previous work showed that the onset potential and peak current density of formic acid electro-oxidation on Pd is *ca.* 100 mV more negative and 2 mA mg⁻¹ (at 0.27 V) higher than that on Pt in the cyclic voltammetry and chronoamperometry tests, respectively.⁴² Therefore, in the present work, we prepared carbon supported Pd nanoparticles (Pd/C) as an anode catalyst for a DFAFC to self-sustainably remove formic acid remaining in the downstream of ECH of LA + FA. The electrocatalytic oxidation (removal) of FA was performed by continuously cycling the effluent of a FA-VA mixture in a H₂SO₄ solution (50 ml) into the anode chamber of DFAFC at 1.0 ml min⁻¹ for 6 hours. A constant fuel-cell voltage of 0.1 V was applied by controlling the outer-circuits resistance to cogenerate electrical energy. As shown in Fig. 5(a), fed with 1.0 M FA + 0.3 M VA of 0.5 M H₂SO₄ solution, the current density drops to 17.8 mA cm⁻² from its initial value (218.6 mA cm⁻²) after 6 hours operation; meanwhile 47% of the FA present in the reactant mixture has been electrocatalytically removed (Fig. 5(b)). It is interesting to note that our independent experiment conducted by feeding 0.3 M VA + 0.5 M H₂SO₄ into the fuel cell produces a current density of <0.1 mA cm⁻² under identical operation conditions, indicating the inertness of VA over the Pd/C anode catalyst (Fig. S1†). The measured concentration of VA remains close to 90%, shown in Fig. 5(b), as compared with its normalized concentration at the beginning of the reaction. The small loss of VA after 6 hours reaction may be due to its evaporation, and could be minimized by optimizing future fuel cell reactor design. In addition, it is worthwhile to mention that the difference of total electrons calculated by integrating the total generated charges from FA electro-oxidation using the coulometer

in the fuel cell tester and by counting the converted FA assuming that two-electron transfer to CO₂ is less than 2%, which suggests a satisfactory experiment accuracy of our electrochemical and analytical methods. In order to investigate the effect of added VA on FA electro-oxidation, 1.0 M FA alone with 0.5 M H₂SO₄ was fed into the DFAFC. Fig. 5(a) shows that in the absence of VA, the current density also gradually decreased and stabilized at 17.5 mA cm⁻² because the reaction rate would decrease with more FA converted. However, the conversion of FA can reach 69% after 6 hours reaction, which is higher than that with VA added in the solution (Fig. 5(b)). The presence of VA in the solution appears to inhibit the FA electro-oxidation rate over Pd/C, resulting in low current density at fuel cell operation at 0.1 V.

The polarization and power density curves of DFAFC with two different fuels are shown in Fig. 6. When fed with 1.0 M FA + 0.5 M H₂SO₄ at a flow rate of 1.0 ml min⁻¹, the DFAFC with a loading of 3.0 mg_{Pd} cm⁻² yielded an open circuit

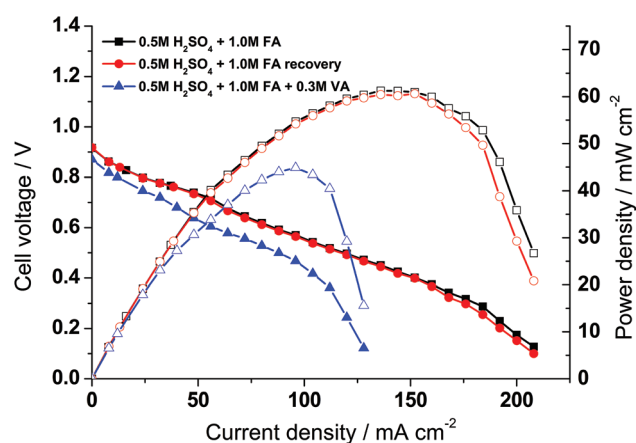


Fig. 6 Polarization and power density curves of a DFAFC employing Pd/C-40 wt% anode catalyst without and with VA addition and after DI water washing recovery. Anode fuel: 1 ml min⁻¹, cathode: O₂, 400 ml min⁻¹, ambient pressure, 30 °C.

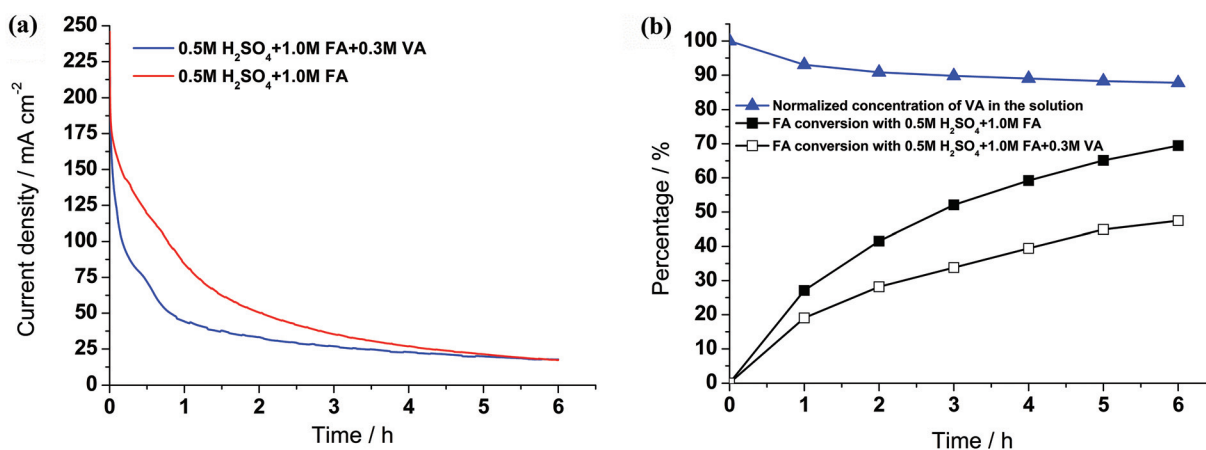


Fig. 5 (a) Current density and (b) FA conversion and normalized concentration of VA as a function of time for electro-oxidation of FA in a DFAFC. Reaction conditions: constant fuel cell voltage of 0.1 V; anode: 1 ml min⁻¹, Pd/C-40 wt%, 3.0 mg_{Pd} cm⁻²; cathode: O₂, 400 ml min⁻¹, ambient pressure, Pt/C-40 wt%, 3.0 mg_{Pt} cm⁻²; 30 °C.

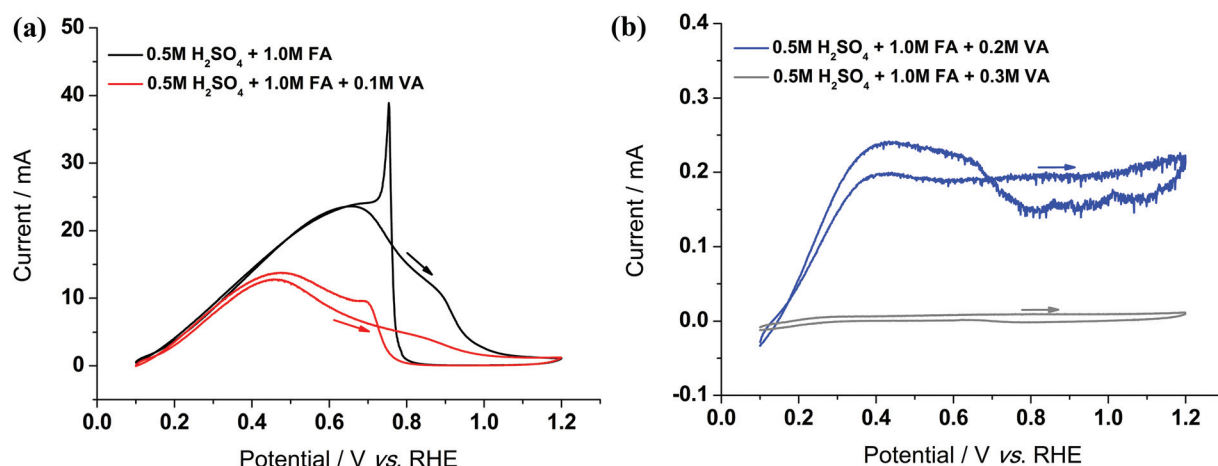


Fig. 7 Cyclic voltammograms of Pd/C-40 wt% catalyst in (a) 0 M, 0.1 M, (b) 0.2 M or 0.3 M VA + 1.0 M formic acid + 0.5 M H_2SO_4 solution, at 50 mV s^{-1} , room temperature.

voltage (OCV) of 0.92 V and a peak power density of 61.3 mW cm^{-2} (at 135.9 mA cm^{-2}) at 30°C . However, with the addition of 0.3 M VA, this DFAFC only produced an OCV of 0.87 V and its peak power density drops to 44.9 mW cm^{-2} (at 95.9 mA cm^{-2}). The observed inhibition of Pd/C electro-catalysts by a VA-FA mixture fuel can be further evidenced by the decrease of the limiting current density from 208.1 mA cm^{-2} to 127.9 mA cm^{-2} , which implies poor fuel diffusion due to the presence of VA in the electrolyte. However, after the 6 hours reaction, the membrane electrode (MEA) was cleaned by washing with copious deionized water until no VA was detected in the filtrate. The polarization and power density curves of the DFAFC with the recovered MEA were collected again by feeding 1.0 M FA + 0.5 M H_2SO_4 . As shown in Fig. 6, nearly repeated I - V curves indicate no fuel cell performance drop between the fresh MEA and its recovery with DI water washing, indicating that the negative effect of VA on FA electro-oxidation is a reversible process, the Pd/C anode catalyst is highly stable and the DFAFC performance can be recovered with DI water washing.

To study the VA effects on the electrocatalytic oxidation of FA over Pd/C, various concentrations of VA ranging from 0.1 M to 0.3 M was added to 1.0 M FA + 0.5 M H_2SO_4 and the cyclic voltammetry (CV) experiment was performed on Pd/C in a half cell. Fig. 7 shows that the peak currents for FA electro-oxidation in the presence of 0.1 M and 0.2 M VA are 12.7 mA and 0.22 mA, respectively, which are 46% and 99% lower than the original current of 23.6 mA. As the VA concentration is increased to 0.3 M, hardly any anodic current can be observed. To confirm that the decreased current is not attributed to the competitive electro-oxidation of VA, blank CV experiments with different VA concentrations of 0.1 M, 0.2 M, and 0.3 M were conducted under identical test conditions in 0.5 M H_2SO_4 aqueous solution. Compared with the cyclic voltammogram of a blank 0.5 M H_2SO_4 , there is nearly no anodic current generated from VA oxidation on Pd/C in the course of the CV scan (0.1 V to 1.2 V) (Fig. 8), which agrees well with the negligible current density observed when 0.3 M VA + 0.5 M H_2SO_4 fed into the DFAFC (Fig. S1†). Therefore, the product VA from ECH

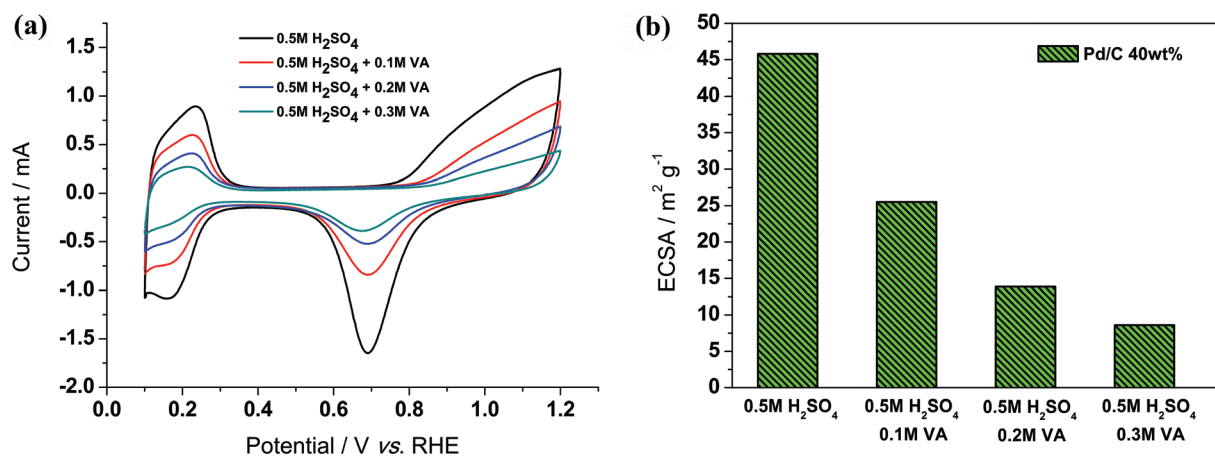


Fig. 8 (a) Cyclic voltammograms and (b) ECSA of Pd/C-40 wt% catalyst in 0 M, 0.1 M, 0.2 M or 0.3 M VA + 0.5 M H_2SO_4 solution, at 50 mV s^{-1} , room temperature.

of LA clearly suppresses the electro-oxidation of FA over Pd/C in the DFAFC reactor, which is integrated to electrocatalytically oxidize (remove) FA to refine the VA biofuel intermediate. It is also noted in Fig. 8 that the degree of inhibition is directly correlated to the concentration of VA presented in the FA sulfuric solution. In contrast to the CV curve recorded in blank 0.5 M H_2SO_4 , both the hydrogen desorption and PdO reduction peaks are reduced with the increase of VA concentration. The electrochemical surface area (ECSA) is calculated by quantification of the electric charges associated with the reduction of the surface PdO layer. The upper potential bound of 1.2 V vs. RHE corresponds to a charge density of around $300 \mu\text{C cm}^{-2}$,⁴³ leading to ECSA of $45.8 \text{ m}^2 \text{ g}^{-1}$ in 0.5 M H_2SO_4 . When the VA concentration was increased from 0.1 M to 0.3 M, the ECSA of Pd/C drops to 25.5 and $8.6 \text{ m}^2 \text{ g}^{-1}$, respectively, as depicted in Fig. 8. The loss of ECSA indicates that the catalytic active sites have been blocked by VA *via* its carboxylic group adsorption.

To further investigate how VA inhibited the electro-oxidation of FA, various carboxylic acids (0.2 M acetic acid, propionic acid, butyric acid and VA) with different alkyl group sizes (from C_2 to C_5) were added to the 1.0 M FA + 0.5 M H_2SO_4 solution. Compared with the CV curve of blank 0.5 M H_2SO_4 , it is noted in Fig. 9 that the C_2 – C_5 carboxylic acids present in the electrolyte, despite showing no activity on Pd/C, significantly reduce the ECSA of the Pd catalyst. Moreover, upon the increase of the carbon chain length from C_2 to C_5 , the ECSA loss of Pd/C becomes more severe. For example, when 0.2 M acetic acid (C_2 carboxylic acid) is added, ECSA drops to $35.8 \text{ m}^2 \text{ g}^{-1}$ (22% decrease from the original ECSA), and it decreases to 30.9, 24.1, and $13.9 \text{ m}^2 \text{ g}^{-1}$ with the addition of 0.2 M propionic acid (C_3), butyric acid (C_4) and VA (C_5), respectively. These results indicate that the anion adsorption of $-\text{COOH}$ in VA is responsible for the inhibition of FA electro-oxidation on Pd/C, and it will prevent formic acid from further oxidation on Pd/C in the DFAFC.

A previous study on the influence of acetate ions on ethanol electro-oxidation on a polycrystalline platinum electrode

demonstrated that the accumulation of the product acetic acid in the electrolyte will lead to acetate anions adsorbed on the platinum electrode, which will compete with ethanol adsorption, thus significantly impeding ethanol oxidation in direct ethanol fuel cells.⁴⁴ It appears similar to the aforementioned findings of the blocking effect of alkyl carboxylic acids. In addition, an alkyl group linked to $-\text{COOH}$ tends to donate electrons to carboxylic ions, and based on density function theory (DFT) calculation, the electronegativity of alkyl groups, being electron releasing, was found to decrease with the increase of the length of the alkyl chain.⁴⁵ Therefore, the electro-donating effect of the alkyl group will increase the electron density of carboxylic ions, making it destabilized, and readily coordinate with the metallic electrocatalysts, such as Pd/C and Pt/C (Fig. S2–S4†). Also, the long carbon chains will also entangle each other to prevent the FA diffusion to the catalyst surface for the electro-oxidation reaction.

In summary, it is promising that FA conversion of 47% can be achieved in 6 hours of electro-oxidation of FA–VA H_2SO_4 solution in DFAFC, and the VA present is inert to the Pd/C anode catalyst. However, the results also suggest that Pt-group metal catalysts used for electrocatalytic conversion of FA cannot tolerate the impurities of carboxylic acid with long alkyl chains.

Challenges and prospects of electrocatalytic biorefinery of raw biomass feedstock to biofuel/intermediates

Electrochemical potential applied at the aqueous/metal interface can lead to significant changes in the reaction thermodynamics, kinetics and mechanisms as compared to traditional heterogeneous chemical catalysis.⁴⁶ Further, renewable electricity generation^{47–49} and storage^{28,30,50} can be directly achieved through electrocatalytic processes. Therefore, electrocatalysis is expected to play a more important role in green, sustainable and cost-effective biomass conversions and biofuel productions.⁵¹ Electrocatalytic processing of biomass feedstock is considered a green route to sustainable production of fuels and chemicals. However, most of the previous research on electrocatalytic oxidation and hydrogenation has been

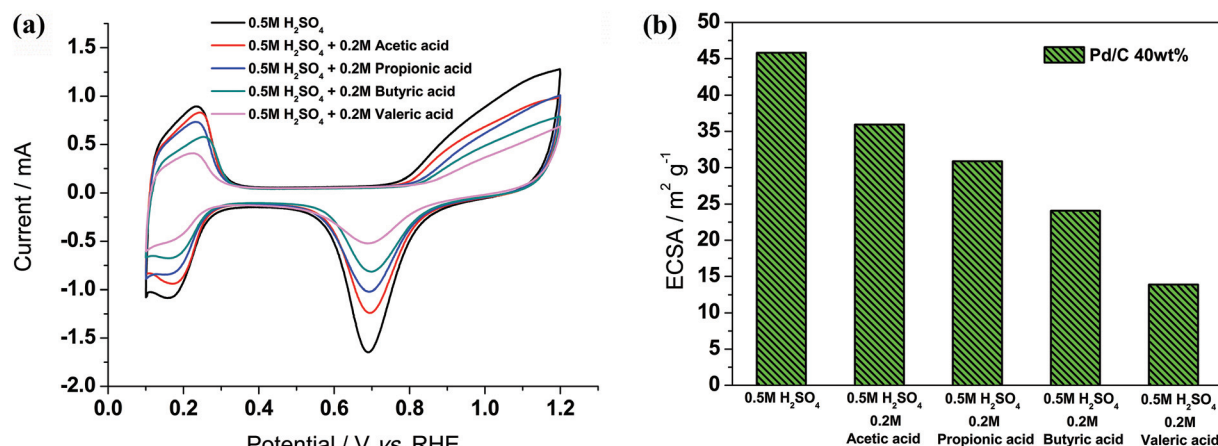


Fig. 9 (a) Cyclic voltammograms and (b) ECSA of Pd/C-40 wt% catalyst in 0.2 M acetic acid, propionic acid, butyric acid or valeric acid + 0.5 M H_2SO_4 solution, at 50 mV s^{-1} , room temperature.

focused on “pure” biomass platform compounds. It is well known that most biorefinery downstreams are often very complex, containing lots of components besides the main targeted feedstock compound. There is an increasing need to explore green electrocatalytic routes to directly process the biorefinery streams to fuels and chemicals, but the effects of the “impurities” (the coupled components) in the biorefinery streams, such as adsorption and catalytic behaviour, on the electrocatalysts must be investigated first. To this end, we made efforts at electrocatalytic processing of simulated real levulinic acid feedstock from acid-catalyzed cellulose hydrolysis, and have found that small formic acid has no negative effects on the electro-hydrogenation of LA, but chain carboxylic acids with different lengths of carbon chains will affect the electro-oxidation of FA.

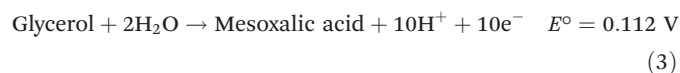
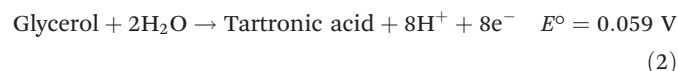
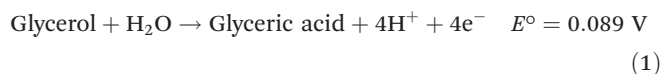
Regarding renewable electricity utilization, environmental conservation and economic feasibility, the presented electrocatalytic hydrogenation mitigates several concerns associated with the conventional heterogeneous catalytic hydrogenation of biomass-derived oxygenates, which are, in most cases, the demand for external pressurized hydrogen, elevated temperatures and energy-intensive separation processes. The presented electrocatalytic biorefining strategy integrates electrocatalytic hydrogenation and electrocatalytic oxidation processes, through which the aqueous solution containing LA and FA derived from acid-catalyzed hydrolysis upstream of waste cellulosic materials can be sustainably converted to biofuel intermediates, such as VA. It has obvious advantages as discussed below: (1) Overproduced renewable electricity (*e.g.* generated from wind turbines, solar panels, tidal power, *etc.*) can be directly used to drive the electro-reduction reaction, and stored in liquid fuels/fuel intermediates with higher energy density, which fits into the existing robust liquid fuel transportation infrastructure. (2) The high pressure hydrogen gas (10–30 bar) and high temperature (370–420 K)⁸ required for the conventional catalytic system are not needed, since atomic hydrogen can be generated *in situ* on the catalytic electrode, and the energy barriers for different elementary reaction steps can be overcome by controlling the electrode potential in the single electrocatalytic flow cell reactor. Therefore, the operating cost can be reduced due to the simplicity of the electrocatalytic reactor design and operation. (3) The VA/FA mixture solution produced from LA electro-hydrogenation can be fed into the anode compartment of a DFAFC to self-sustainably remove the FA.

Although the single electrocatalytic flow cell reactor in conjunction with DFAFC presented in this work could be potentially profitable and environmentally friendly as compared with the conventional catalytic processes, challenges to make this integrated electrocatalytic system more practical still exist. It is reported that a higher reaction rate achieved has to be at a sacrifice of an input energy increase and thus higher overpotentials (>1.0 V) are needed to produce sufficient atomic hydrogen over a Pb electrode to trigger the ECH reaction, as well as overcome the activation energy of the electro-hydrogenation reaction. One method to improve the efficiency of the overall reaction is to replace the bulk electrode by

incorporating the nanostructured metallic catalysts into the membrane electrode assembly (MEA). Recently, interesting research has been conducted to enhance the kinetics for the electro-hydrogenation reaction on the nano-catalysts. For example, the reduction of lactic acid and bio-oil derived phenolic compounds using supported Ru nanoparticles has been investigated in a one-compartment electrolysis cell and two-chamber standard glass H-cell, respectively.^{29,40,52} The Huber group performed the electrocatalytic hydrogenation of acetone and furfural over Pt/C and Pd/C in a PEM-based continuous reactor.^{28,39} All of these studies have supported that the ECH of oxygenate compounds on nanostructured catalysts in the single electrocatalytic flow cell reactor is promising in terms of reaction rate and energy efficiency.

Another challenge is the observed serious catalyst deactivation issue associated with electrocatalytic oxidation of FA in a DFAFC; this is mainly due to the presence of VA – a primary alkyl-carboxylic acid, which can act as an electron donor occupying the noble metal catalytic active sites for FA oxidation. We also find that the strength of the alkyl-carboxylic acid interacting with the electro-catalysts depends on the number of carbons in the alkyl group along with the properties of metallic catalysts used. Therefore, theoretical and experimental work is needed in the future to screen the proper catalysts and rationally design more efficient catalysts so as to weaken the interaction between the alkyl-carboxylic group and metal *via* electronic structure manipulation.

Alternative reactor design could also help to minimize the energy cost. One wise option may be to couple electro-oxidation of biorenewable compounds to valuable chemicals at the anode of the single electrocatalytic flow cell reactor. This is because of the relatively high theoretical voltage (1.229 V *vs.* SHE) needed for the current coupled oxygen evolution reaction (oxidation of water) occurring in the anode compartment of the single electrocatalytic flow cell reactor. Electro-oxidation of biomass-derived polyols, such as glycerol, to glyceric acid, tartronic acid and mesoxalic acid needs only 0.089 V, 0.059 V and 0.112 V *vs.* SHE, respectively. These partial oxidation products have higher value and broader market applications than glycerol, and their selectivity can be well regulated by appropriately tuning the applied potential as we have demonstrated before.⁵³ Thus, it is more economically favorable to electro-hydrogenate LA at the cathode by protons generated from a renewable alcohol oxidation at the anode.



Additionally, the single electrocatalytic flow cell reactor could be further improved by cycling the cathodic effluent that

consists of VA and FA to the inlet of the anodic compartment for on-stream removal of FA. This new approach will integrate the 2-step operation in a single electrocatalytic flow cell reactor powered by renewable electrical energy, achieving the LA reduction and FA oxidation simultaneously, thereby minimizing the material and energy costs.

Conclusions

In this work, we investigated the downstream of acid-catalyzed cellulose hydrolysis as a feedstock for an integrated electrocatalytic process that couples the ECH of LA + FA in a single electrocatalytic flow cell reactor and electrocatalytic oxidation of FA in a DFAFC. The investigations on ECH of LA + FA in H_2SO_4 aqueous solution to VA and gVL on a Pb electrode in the single electrocatalytic flow cell reactor show that high selectivity to VA (>90%) and high Faradaic efficiency (>47%) can be maintained during 8 hours of reaction. It was also clearly demonstrated that the presence of FA in the LA aqueous solution is stable and has been found to have no negative effect in terms of LA conversion, ECH reaction rate and Faradaic efficiency. When 1.0 M FA + 0.3 M VA was directly fed into DFAFC, 47% FA conversion was achieved in 6 hours and VA is inert to the Pd/C anode catalyst during the FA electro-oxidation reaction. However, Pd/C was found to be reversibly deactivated by VA in the reactant mixtures. The half-cell tests demonstrated that higher VA concentration leads to more serious competition with FA for electrochemical active sites of Pd/C. In addition, carboxylic acids with different lengths of alkyl chains (C_2 to C_5) were explored under the FA electro-oxidation conditions and these compounds with longer carbon chains apparently adsorbed stronger onto Pd/C, resulting in a lower ECSA. The results suggest that the proposed integrated electrocatalytic biorefinery process, though very promising, currently remains challenging. Advanced electrocatalytic materials that can tolerate impurities existing in the streams of a crude biomass process need to be developed, and coupling important electrocatalytic transformations of biomass-compounds can be further optimized to minimize the overall material and energy costs.

Experimental

Proton exchange membrane (PEM)-single electrocatalytic flow cell reactor study

The single electrocatalytic flow cell reactor is custom-designed with a Pb electrode (Aldrich Chemistry, 99.99%) of 5 mm thickness as the working (cathode) electrode, while a Pt foil (Aldrich Chemistry, 99.99%) with an active area of 5 cm^2 serves as the counter (anode) electrode.³⁰ A proton-exchange membrane (Nafion N117, Ion Power, Inc.) was used to separate the anode and cathode chambers. Levulinic acid of 0.2 M, 0.5 M and 1.0 M with or without an equal concentration of formic acid in 0.5 M H_2SO_4 was fed into the cathode chamber in a closed loop by a peristaltic pump (Gilson Miniplus 3), while

0.5 M H_2SO_4 aqueous solution was quickly pumped into the anode chamber to remove the O_2 that was produced during the oxygen evolution reaction (OER) on the Pt foil electrode. The applied potential at the cathode was controlled at -1.5 V vs. RHE via a potentiostat (VersaSTAT MC, Princeton Applied Research). The products collected at each hour were analysed by HPLC.

Preparation and physical characterization of the Pd/C catalyst

The Pd/C catalyst was synthesized by a modified organic solution phase reduction method, and has been reported elsewhere.^{54,55} Briefly, 152.3 mg of $\text{Pd}(\text{acac})_2$ (0.5 mmol, Aldrich Chemistry, 97%) and 79.8 mg of Vulcan XC-72R carbon black (Cabot) were mixed in 40 ml benzyl ether (Alfa Aesar, 98%) solvent and rapidly heated up to 100°C under a nitrogen flow. As the temperature reached 100°C , 200 μl of oleylamine (Aldrich Chemistry, 70%) and 200 μl of oleic acid (Aldrich Chemistry, 90%) were injected into the system, followed by a quick injection of 1.0 ml LiBet_3H (1 M in THF, Acros Organics). After holding at 100°C for 30 min, the temperature was slowly ramped to 180°C and kept for an additional 1 hour. The Pd/C catalyst was collected by filtration, washed with copious ethanol, and dried in a vacuum oven at 50°C overnight. The ca. 40 wt% metal loading of Pd/C was determined by using ICP-AES as well as by measuring the weight differences between the initial input of carbon black and the final Pd/C catalyst. X-ray diffraction (XRD) patterns shown in Fig. S5† were collected on a Scintag XDS-2000 θ/θ diffractometer with $\text{Cu K}\alpha$ radiation ($\lambda = 1.5406 \text{ \AA}$), with a tube current of 35 mA and a tube voltage of 45 kV. The transmission electron microscopy (TEM) characterization (Fig. S6†) was conducted on a JEOL JEM-4000FX with an operation voltage of 200 kV.

Proton exchange membrane-direct formic acid fuel cell (DFAFC) study

The fuel cell tests were performed on a Scribner Fuel Cell System 850e (Scribner Associates, USA), and the fuel cell fixture with an active area of 5 cm^2 was purchased from Fuel Cell Technology Inc. They have been used well in our previous single fuel cell study.^{49,53–55,57} The anode electrode composed of 70 wt% Pd/C catalyst and 30 wt% Nafion ionomer was sprayed onto a PTFE-untreated carbon cloth liquid diffusion layer to obtain a catalyst loading of $3.0 \text{ mg}_{\text{Pd}} \text{ cm}^{-2}$. At the cathode, catalyst slurry containing 70 wt% of Pt/C (Fuel Cell Store, 40 wt%) and 30 wt% of Nafion ionomer was sprayed onto a PTFE-treated carbon cloth gas diffusion layer to obtain a catalyst loading of $3.0 \text{ mg}_{\text{Pt}} \text{ cm}^{-2}$. Finally, a 5 wt% Nafion solution was sprayed onto the surface of both the anode and the cathode ($1.0 \text{ mg Nafion cm}^{-2}$) to form a thin Nafion layer. The membrane electrode assembly (MEA) was constructed by hot pressing the anode, the cathode and the pre-treated Nafion membrane (N117, Ion Power, Inc.) under a pressure of 140 atm at 135°C for 3 min.⁵⁶ 1.0 M formic acid with or without the addition of 0.3 M valeric acid in 0.5 M H_2SO_4 was pumped into the anode compartment at 1 ml min^{-1} , while high purity O_2 (99.999%) regulated at 400 ml min^{-1} was fed

into the cathode compartment under ambient pressure. The polarization curves of the DFAFC were collected by scanning current at 30 °C. Electrocatalytic oxidation of FA was performed for 6 hours at a fuel cell voltage of 0.1 V. Samples were withdrawn every 1 h and analysed by HPLC.

Half-cell study

Half-cell tests were performed in a conventional single compartment three electrode-cell setup (electrochemical cell AFCELL3, Pine Instrument) with a glassy carbon (GC) working electrode, a reversible hydrogen reference electrode (Hydroflex®) reference electrode, and a Pt wire counter electrode. All testing electrolytes were de-aerated with high purity N₂ (99.999%) for 30 min before use. Prior to the experiments, 2.0 mg Pd/C was ultrasonically dispersed in 1.0 ml isopropanol and 10 µl of Nafion solution (5 wt%, 1100 EW, Ion Power, Inc.) to form uniform ink. 80 µl of the catalyst ink was drop-casted onto the GC electrode. The activity of formic acid electro-oxidation on Pd/C was measured by carrying out cyclic voltammetry (CV) in 0.5 M H₂SO₄ aqueous solution mixed with 1.0 M formic acid or 1.0 M formic acid + valeric acid (0.1–0.3 M) in the potential region between 0.1 V and 1.2 V (vs. RHE) at a scan rate of 50 mV s⁻¹, 25 °C and 2000 rpm. CVs recorded in the same potential window using either blank 0.5 M H₂SO₄ or 0.5 M H₂SO₄ with different carboxylic acids, including acetic acid, propionic acid, butyric acid and valeric acid, were employed to determine the electrochemical surface area (ECSA) change. Twenty cyclic voltammograms were recorded under each condition and the final CV is reported in this paper.

Product analysis

A high performance liquid chromatography instrument (HPLC, Agilent 1100), equipped with a refractive index detector (RID, Agilent G1362A) and a variable wavelength detector (VWD, Agilent G1314A, 220 nm), was used to quantify the products from the levulinic acid electro-hydrogenation reaction and the formic acid electro-oxidation reaction carried out in the single electrocatalytic flow cell reactor and the DFAFCs reactor, respectively. An OA-1000 column (Alltech, 60 °C) with an eluent of 5 mM aqueous sulfuric acid (0.3 ml min⁻¹) was applied for the product separation. 20 µl of each sample was injected into the HPLC system. All products were identified by comparison with the authentic samples. Carbon balances were calculated based on our previously reported method,³⁰ and are close to within 10% for all experiments reported here.

The product yield was calculated from eqn (4):

$$\text{Products yield (\%)} = \text{Selectivity} \times \text{Conversion} \quad (4)$$

The Faradaic efficiency was defined by eqn (5):

$$\text{Faradaic efficiency} = \frac{\sum(\text{mol}_i \times n_i) \times F}{I \times t} \times 100\% \quad (5)$$

where n is the number of electrons transferred, F is the Faraday constant, I is the current observed in the experiment, and t is the duration of the experiment.

Acknowledgements

We acknowledge financial support from the US National Science Foundation (CBET-1032547 and CBET-1235982). J.Q. is grateful to the Chinese Scholarship Council for support.

References

- 1 W. S. Broecker, T. Takahashi, H. J. Simpson and T. H. Peng, *Science*, 1979, **206**, 409–418.
- 2 S. J. Davis, K. Caldeira and H. D. Matthews, *Science*, 2010, **329**, 1330–1333.
- 3 R. W. Dudley, *BP Energy Outlook 2030*, BP Statistical Review, London, 2011.
- 4 G. W. Huber, *Breaking the chemical and engineering barriers to lignocellulosic biofuels: next generation hydrocarbon biorefineries*, NSF, ACS and US-DOE Workshop report, Washington D.C., 2007.
- 5 P. Meisen, *Renewable Energy Potential of Latin America*, Global Energy Network Institute (GENI), San Diego, California, 2009.
- 6 P. Meisen, *Renewable Energy Potential of China: Making the Transition from Coal-Fired Generation*, Global Energy Network Institute (GENI), San Diego, California, 2009.
- 7 A. J. Ragauskas, C. K. Williams, B. H. Davison, G. Britovsek, J. Cairney, C. A. Eckert, W. J. Frederick, J. P. Hallett, D. J. Leak, C. L. Liotta, J. R. Mielenz, R. Murphy, R. Templer and T. Tschaplinski, *Science*, 2006, **311**, 484–489.
- 8 C. H. Zhou, X. Xia, C.-X. Lin, D.-S. Tong and J. Beltramini, *Chem. Soc. Rev.*, 2011, **40**, 5588–5617.
- 9 G. W. Huber, S. Iborra and A. Corma, *Chem. Rev.*, 2006, **106**, 4044–4098.
- 10 S. M. Sen, D. M. Alonso, S. G. Wettstein, E. I. Gurbuz, C. A. Henao, J. A. Dumesic and C. T. Maravelias, *Energy Environ. Sci.*, 2012, **5**, 9690–9697.
- 11 S. M. Sen, E. I. Gurbuz, S. G. Wettstein, D. M. Alonso, J. A. Dumesic and C. T. Maravelias, *Green Chem.*, 2012, **14**, 3289–3294.
- 12 J. J. Bozell and G. R. Petersen, *Green Chem.*, 2010, **12**, 539–554.
- 13 L. E. Manzer, *Biomass Derivatives: A Sustainable Source of Chemicals*, National Science Foundation Workshop: Catalysis for Renewables Conversion, Arlington, VA, 2004.
- 14 J. J. Bozell, L. Moens, D. C. Elliott, Y. Wang, G. G. Neuenschwander, S. W. Fitzpatrick, R. J. Bilski and J. L. Jarnefeld, *Resour., Conserv. Recycl.*, 2000, **28**, 227–239.
- 15 G. Kulesa, *Manufacture of Industrial Chemical From Levulinic Acid: A New Feedstock For The Chemicals Industry*, Chemical Project Fact Sheet, U.S. Department of Energy, Washington, D.C., 1999.
- 16 W. R. H. Wright and R. Palkovits, *ChemSusChem*, 2012, **5**, 1657–1667.

- 17 L. Deng, Y. Zhao, J. Li, Y. Fu, B. Liao and Q. X. Guo, *ChemSusChem*, 2010, **3**, 1172–1175.
- 18 S. G. Wettstein, J. Q. Bond, D. M. Alonso, H. N. Pham, A. K. Datye and J. A. Dumesic, *Appl. Catal., B*, 2012, **117**, 321–329.
- 19 D. J. Braden, C. A. Henao, J. Heltzel, C. T. Maravelias and J. A. Dumesic, *Green Chem.*, 2011, **13**, 1755–1765.
- 20 J. C. Serrano-Ruiz, D. Wang and J. A. Dumesic, *Green Chem.*, 2010, **12**, 574–577.
- 21 J. Q. Bond, D. M. Alonso, D. Wang, R. M. West and J. A. Dumesic, *Science*, 2010, **327**, 1110–1114.
- 22 D. M. Alonso, S. G. Wettstein, M. A. Mellmer, E. I. Gurbuz and J. A. Dumesic, *Energy Environ. Sci.*, 2013, **6**, 76–80.
- 23 J. C. Serrano-Ruiz, D. J. Braden, R. M. West and J. A. Dumesic, *Appl. Catal., B*, 2010, **100**, 184–189.
- 24 E. I. Guerbuez, D. M. Alonso, J. Q. Bond and J. A. Dumesic, *ChemSusChem*, 2011, **4**, 357–361.
- 25 P. M. Ayoub, WO/2005/070867, 2005.
- 26 X. L. Du, Q. Y. Bi, Y. M. Liu, Y. Cao and K. N. Fan, *ChemSusChem*, 2011, **4**, 1838–1843.
- 27 S. Saravanamurugan, O. Nguyen Van Buu and A. Riisager, *ChemSusChem*, 2011, **4**, 723–726.
- 28 S. K. Green, G. A. Tompsett, H. J. Kim, W. B. Kim and G. W. Huber, *ChemSusChem*, 2012, **5**, 2410–2420.
- 29 Z. L. Li, M. Garedew, C. H. Lam, J. E. Jackson, D. J. Miller and C. M. Saffron, *Green Chem.*, 2012, **14**, 2540–2549.
- 30 L. Xin, Z. Zhang, J. Qi, D. J. Chadderton, Y. Qiu, K. M. Warsko and W. Li, *ChemSusChem*, 2013, **6**, 674–686.
- 31 S. Ha, R. Larsen, Y. Zhu and R. I. Masel, *Fuel Cells*, 2004, **4**, 337–343.
- 32 S. Ha, R. Larsen and R. I. Masel, *J. Power Sources*, 2005, **144**, 28–34.
- 33 Z. L. Liu, L. Hong, M. P. Tham, T. H. Lim and H. X. Jiang, *J. Power Sources*, 2006, **161**, 831–835.
- 34 X. Wang, Y. Tang, Y. Gao and T. Lu, *J. Power Sources*, 2008, **175**, 784–788.
- 35 C. Jung, C. M. Sánchez-Sánchez, C.-L. Lin, J. n. Rodríguez-López and A. J. Bard, *Anal. Chem.*, 2009, **81**, 7003–7008.
- 36 Z. Liu and X. Zhang, *Electrochem. Commun.*, 2009, **11**, 1667–1670.
- 37 J. L. Haan, K. M. Stafford, R. D. Morgan and R. I. Masel, *Electrochim. Acta*, 2010, **55**, 2477–2481.
- 38 M. Yin, Q. Li, J. O. Jensen, Y. Huang, L. N. Cleemann, N. J. Bjerrum and W. Xing, *J. Power Sources*, 2012, **219**, 106–111.
- 39 S. K. Green, J. Lee, H. J. Kim, G. A. Tompsett, W. B. Kim and G. Huber, *Green Chem.*, 2013, **15**, 1869–1879.
- 40 T. S. Dalavoy, J. E. Jackson, G. M. Swain, D. J. Miller, J. Li and J. Lipkowski, *J. Catal.*, 2007, **246**, 15–28.
- 41 J.-M. Saveant, *Chem. Rev.*, 2008, **108**, 2348–2378.
- 42 O. Winjobi, Z. Zhang, C. Liang and W. Li, *Electrochim. Acta*, 2010, **55**, 4217–4221.
- 43 T. Chierchie, C. Mayer and W. J. Lorenz, *J. Electroanal. Chem.*, 1982, **135**, 211–220.
- 44 S. Gilman, *Electrochim. Acta*, 2012, **65**, 141–148.
- 45 F. De Proft, W. Langenaeker and P. Geerlings, *Tetrahedron*, 1995, **51**, 4021–4032.
- 46 M. J. Janik, S. A. Wasileski, C. D. Taylor and M. Neurock, in *Fuel Cell Catalysis: A Surface Science Approach*, ed. M. T. M. Koper, John Wiley & Sons, New York, 2008, ch. 4.
- 47 C. Lamy, E. M. Belgsir and J. M. Leger, *J. Appl. Electrochem.*, 2001, **31**, 799–809.
- 48 A. Kowal, M. Li, M. Shao, K. Sasaki, M. B. Vukmirovic, J. Zhang, N. S. Marinkovic, P. Liu, A. I. Frenkel and R. R. Adzic, *Nat. Mater.*, 2009, **8**, 325–330.
- 49 Z. Y. Zhang, L. Xin and W. Z. Li, *Appl. Catal., B*, 2012, **119**, 40–48.
- 50 P. Nilges, T. R. dos Santos, F. Harnisch and U. Schroder, *Energy Environ. Sci.*, 2012, **5**, 5231–5235.
- 51 R. A. van Santen, in *Catalysis for Renewables: From Feedstock to Energy Production*, ed. G. Centi and R. A. van Santen, John Wiley & Sons, New York, 2007, ch. 1.
- 52 Z. L. Li, S. Kelkar, C. H. Lam, K. Luczek, J. E. Jackson, D. J. Miller and C. M. Saffron, *Electrochim. Acta*, 2012, **64**, 87–93.
- 53 L. Xin, Z. Zhang, Z. Wang and W. Li, *ChemCatChem*, 2012, **4**, 1105–1114.
- 54 Z. Zhang, L. Xin, K. Sun and W. Li, *Int. J. Hydrogen Energy*, 2011, **36**, 12686–12697.
- 55 Z. Zhang, L. Xin, J. Qi, D. J. Chadderton and W. Li, *Appl. Catal., B*, 2013, **136–137**, 29–39.
- 56 W. Li, C. Liang, W. Zhou, J. Qiu, Z. Zhou, G. Sun and Q. Xin, *J. Phys. Chem. B*, 2003, **107**, 6292–6299.
- 57 J. Qi, L. Xin, Z. Zhang, K. Sun, H. He, F. Wang, D. Chadderton, Y. Qiu, C. Liang and W. Li, *Green Chem.*, 2013, **15**, 1133–1137.